

LUMINESCENCE DATING OF AN ANCIENT WALLED SETTLEMENT IN ORKHON VALLEY, MONGOLIA

Tengis S.^{1*}, Saran S.¹, Munkhbayer L.² and Bemann J.³

¹ Institute of Physics and Technology of the Mongolian Academy of Sciences, Mongolia

² Institute of History and Archaeology of the Mongolian Academy of Sciences, Mongolia

³ Vor- und Frühgeschichtliche Archäologie, Rheinische Friedrich-Wilhelms-Universität Bonn, Germany

*corresponding author, e-mail: tengis@ipt.ac.mn

ARTICLE INFO: Received: 10 Nov, 2017; Revised: 22 Dec, 2017; Accepted: 25 Dec, 2017

Abstract: We investigated the potential of the optically stimulated luminescence (OSL) method to date young (<1000 years) samples collected in the Orkhon Valley Cultural Landscape, Mongolia. Quartz showed an infrared signal; therefore the post-IR OSL method was applied to small aliquots which are considered proxies for single grain measurements. Statistical analysis of the dose distribution produced CAM De of 5.14 ± 0.10 Gy and over dispersion of 47.5%, and MAM De of 3.7 ± 0.6 Gy. Since no partial bleaching was suspected, the analysis of signal composition was done and the fast quartz post-IR OSL lead to De of 4.9 ± 0.2 Gy. Based on the quartz fast component and CAM De we propose the new chronology of ancient construction at 785 ± 80 AD, rather than 906-1125 AD as suggested by archaeological evidence. However, the MAM age is in good agreement with independent age control for construction of the ramparts suggesting the date of reconstruction, collapse or reuse for the square walled enclosure MOR3 during 1090 ± 80 AD.

Keywords: Luminescence; OSL dating; quartz; fast component; Orkhon Valley;

INTRODUCTION

The luminescence technique [2] is based on the fact that many naturally occurring minerals, including quartz and feldspar are able to act as dosimeters for the amount of ionizing radiation they are exposed to. The optically stimulated luminescence (OSL) method dates the last sunlight exposure event for minerals. A basic assumption contained within the OSL approach is that the traps are completely empty of all trapped charge by sunlight during the event, which is being dated. This assumption appears to be the case with ceramics and bricks during the firing process; fired clay brick samples were successfully dated by the thermoluminescence (TL), optically stimulated luminescence (OSL) and

post-infrared stimulated (pIRIR) techniques [21], [24], [20]; using different brick samples they were able to reconstruct the construction of the palatial complex, the palace and the city walls in Karakorum - the ancient capital of the Mongol Empire. However, for construction of walls and ramparts, sediment embedded within the wall may have been incorporated at various stages of the construction process, and from various sources, and may not necessarily have completely reset the OSL signal. In that case scatter in dose distributions of sedimentary samples is expected; the sources are incomplete or heterogeneous bleaching of grains [15]; [7]), post-depositional mixing of grains [18]; [13]; [23] and beta-dose

heterogeneity in the natural burial environment [14]). Several statistical models [10] have been suggested, whose outcome is highly dependent on the uncertainties assigned to individual dose estimates.

Other sources for dispersion of the dose distribution include differences in the OSL signals response from different grains for identical treatments [4]. Internal variability leads to the observation of grains with different luminescence properties, such as brightness, and the presence of quartz grains with different OSL components [3]. For some quartz samples, isolation of the so-called ‘fast component’ of the OSL improves the accuracy of absorbed dose estimates [1]. A quartz fast component [4] is the signal used for D_e evaluation using the single aliquot regenerative–dose protocol by [25]. The ratio of fast to medium component leads to the scatter in D_e distributions [24, 8]. The effect of the medium component on the dose evaluation and the ratio of fast to medium was observed for heated bricks [24].

In this study, we apply OSL dating to the walled enclosure in Orkhon Valley. Small aliquots used as a proxy for single grain measurements were analyzed using two approaches. First, we apply statistical analysis to the post-IR OSL data. Then signal

composition analysis is used to isolate the fast signal dominated dose estimates. The results will be compared and discussed in terms of choosing the appropriate model.

Sampling site

The Orkhon Valley Cultural Landscape includes numerous archaeological remains including Karakorum, the 13th century capital of Mongolia and Karabalgasun, the 8th-9th centuries Uighur capital. In the course of the field work of the German-Mongolian archaeological team in 2009 and 2010, the key region between the supposed spring palace of Ögödei Khan and the urban area of Karabalgasun and its archaeological structures were documented via aerial photograph analysis and ground survey [6]. Altogether 310 archaeological sites were documented in the middle and upper Orkhon Valley; these sites, the majority of which was unknown to archaeologists prior to the project, encompass more than one thousand individual features such as burials, settlements, find scatters, walled enclosure, petroglyphs etc. All periods from the Middle Paleolithic through to Post Medieval and modern times are represented [6].

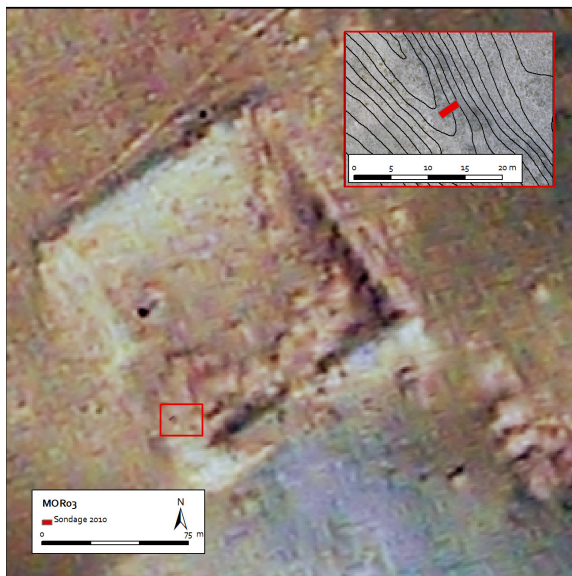


Figure 1. Walled enclosure MOR3 in Orkhon Valley (from [6])

One of this sites is a square walled enclosure (E102°35'33'', N47°28', figure 1) located to the north-west of Karabalgasun presented walled ramparts that were constructed from rammed earth; an ancient method of wall construction using local materials well represented in the Orkhon

Valley. For construction changing layers of sand, clay and gravel were moistened and then pressed into a wooden framework. The rampart itself was constructed in horizontal layers (Fig.2); construction progressing until one layer is complete and compaction of the next layer begins.



Figure 2. Test trench showing the sampling site

The test trench showed that the borders between the bands are very clear-cut which indicated that the rampart was erected from layers of rammed earth. The event to be dated is the preparation of the ramparts. Sample MOR3 was provided with independent age control

suggesting the construction during 906-1125 AD based on archaeological evidence. Clay sediment samples were collected from this ancient settlement in Orkhon Valley for the luminescence dating.

EXPERIMENTAL DETAILS

Sample preparation

Coarse grains ($>100\mu\text{m}$) were treated with 10% HCl to dissolve carbonates, then dispersed using sodium oxalate and 10% H_2O_2 to remove organic material, with a heavy liquid (2.58 g cm^{-3} , 2.62 g cm^{-3} and 2.70 g cm^{-3}) to obtain quartz fractions. Quartz is finally etched with 40% HF for 40 min to remove the alpha irradiated outer rinds of the quartz grains, treated with HCl to remove insoluble fluorides and re-sieved. Coarse grains ($212\mu\text{m}$) were chosen for single grain measurements. Coarse grains ($150\mu\text{m}$) 2mm aliquots were prepared for OSL and post-IR OSL luminescence measurements.

Instrumentation

Luminescence measurements were made on an automated Risø TL/OSL-DA-20 reader equipped with $^{90}\text{Sr}/^{90}\text{Y}$ beta source; with blue diodes ($\sim 470\text{ nm}$) for quartz stimulation. Quartz OSL and TL were detected through a 7.5mm Hoya U-340 filter (290-370 nm) and D_e values were determined using a SAR protocol and a double-SAR protocol.

Single grain measurements were stimulated with a green laser Nd:YVO₄ diode-pumped laser (532 nm) delivering a power density of $\sim 50\text{ W cm}^{-2}$.

OSL measurement

The single-aliquot regenerative-dose (SAR) procedure [25] was used for equivalent dose evaluation. Additionally, a double SAR procedure [5] employed IR stimulation prior to blue stimulation. Fitting of the OSL decay curves was executed using Origin 8.6.

Dose rate measurement

The samples for dose rate determination were dried at 50°C until air dry and finally homogenized. 157 g sample material was filled into a Marinelli beaker and stored for four

weeks to allow equilibrium reestablishment of ^{226}Ra and its daughter nuclides; the samples were analyzed using high-resolution gamma spectrometry. The external and internal dose rates were calculated using the conversion factors [12] and the cosmic dose rates were calculated following Prescott and Hutton [16]. *In situ* water content, measured shortly after sampling, was used to calculate water attenuation factors. The beta-ray attenuation factors were calculated for the grain size of 150 μm .

RESULTS

Dose rate results

The nuclide activities of ^{238}U , ^{232}Th , ^{40}K were converted to dose rates using the

conversion factors given in [12] and shown in Table 1.

Table 1. Radionuclide concentrations

	^{238}U , Bq/kg	^{232}Th , Bq/kg	Ra-U	^{40}K , Bq/kg
MOR3	20.11±1.00	28.21±1.51	20.64±1.36	826.74±8.00

D_e results

The methodology is far more advanced and better understood for quartz in comparison to feldspar and tends to give reliable estimates, however several studies dealing with OSL quartz dating reported problems with low

luminescence efficiency observed most commonly in young samples [17]. To obtain an accurate D_e we investigate the samples using two approaches: statistical analysis and signal composition analysis.

D_e using OSL on quartz

Preliminary green laser stimulated single grain OSL measurements have shown that grains are dim giving around 100 counts; only 4 out of 100 grains gave doses from 1.48±0.33 Gy to 5.15±1.05 Gy. Therefore, small aliquots A small aliquot is an average of up to 100 grains; were used as proxy for single grains

measurements.

Blue stimulated OSL curves are shown in Fig.3. To examine whether the obtained OSL signal originates from more than one electron trap [25], the OSL decay curves were fitted with a sum of exponential components using the equation [22]:

$$I(t) = \sum_{i=1}^N n_i p_i \exp(-p_i t) + c$$

where n_i – concentration of electrons at the i -th trap; p_i – detrapping probability of electrons from the i -th trap; c – constant. The detrapping probability is the product of the photoionization cross-section and the

stimulation intensity.

The fitting results indicate that the fast OSL component and the medium OSL dominate for the initial time period and the slow component is contributing to the overall

signal. Furthermore, the quartz sample with a dominant medium component showed an infrared contaminated signal. The IRSL and

blue stimulated post-IR OSL signals are very similar in intensity.

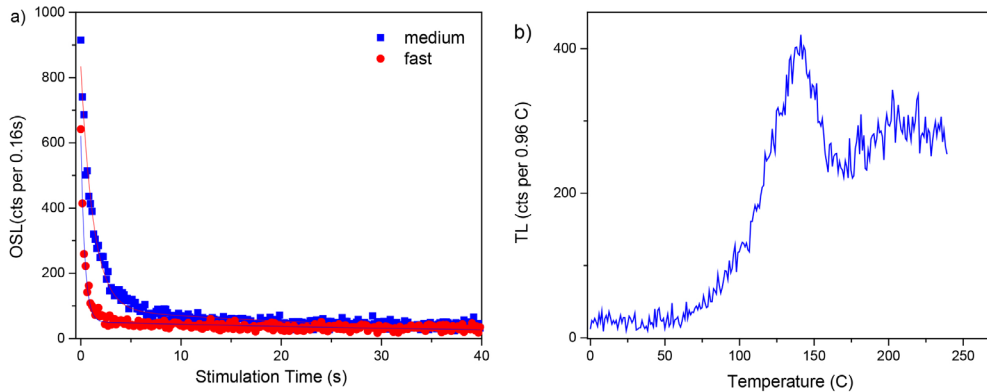


Figure 3. a) OSL signal showing different components; b) TL peaks at 110°C and 200°C; the latter is an indication of presence of feldspar

Table 2. Fitting parameters obtained for two different OSL signals

		fast	medium
fast	n1	220±5	-
	p1, s-1	2.57±0.06	-
medium	n2	-	923±20
	p2, s-1	-	0.80±0.02
slow	n3	3179±216	3392±153
	p3, s-1	0.02±0.001	0.03±0.002

To further investigate the behavior of quartz, the corresponding TL glow curves where the D_e were already evaluated were recorded using small aliquots. Fig.3b shows the TL curves obtained when heating to 450°C, immediately after beta irradiation (4 Gy) and following 10 s preheat at 70°C. The TL glow curves show that there are two dominant TL peaks, one at 110°C and an additional intermediate peak around 200°C was obtained for sample MOR3. It can be speculated that there is a correlation between the presence of an infrared signal and the presence of a significant medium component.

D_e using post-IR OSL on quartz

For MOR3, 24 single aliquots were measured using post-IR OSL which is a technique that stimulates the same aliquot with infra-red (IR) light followed by blue light stimulation [5].

Effect of the precision criteria

The single-aliquot D_e distributions are shown using Abanico plots in Figure 4. The sample showed a broad dose distribution: the D_e varies from ~1 Gy to ~16 Gy. Grain-to-grain variations are assumed to contribute to the D_e scatter.

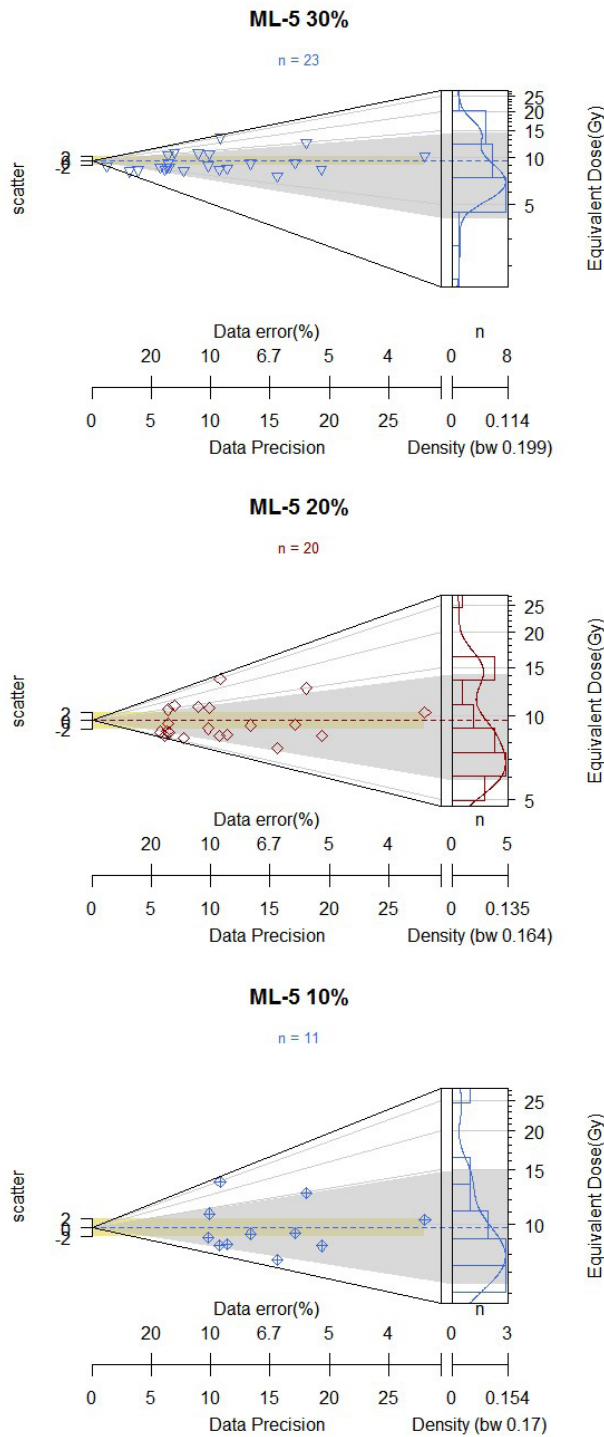


Figure 4. Dose distributions displayed using the Abanico plots for the precision on D_e <30, <20, <10 %

Overdispersion (OD) in a D_e distribution is a quantitative measure that refers to the relative standard deviation of the distribution of true single grain D_e values from a central D_e value, after having allowed for estimation of the statistical error [11]. The choice of model, e.g. central age (CAM), minimum age (MAM) or finite mixture model (FMM) [11], is based on the OD value. This choice assumes that the precision assigned to each D_e measurement is correctly calculated. Many studies have reported up to 20% overdispersion among D_e estimates for single aliquots that have been well bleached [13] [9].

Individual aliquots with precision on $D_e < 30\%$ were analyzed using statistical tools [11], CAM D_e is 5.14 ± 0.54 Gy and overdispersion of 47.5%. MAM D_e was 3.7 ± 0.6 Gy .. The effect of the acceptance

$$\frac{L_x}{T_x} = a \left(1 - \exp \left(-\frac{D}{B} \right) \right)$$

Aliquots with dominant fast component and dominant medium component yield D_e of 4.9 ± 0.2 Gy and 7.39 ± 0.87 Gy, respectively. In concordance with previous speculations, medium OSL component gave higher doses

criteria on dose estimate was analyzed for the precision on $D_e < 20\%$ and $< 10\%$, respectively. With the increase on the precision the number of aliquots decreased from $n=23$ to $n=11$ ($< 10\%$). These precise dose estimates gave CAM D_e of 4.21 ± 0.22 Gy and over dispersion of 17.7%. The CAM and MAM D_e values, the precision on D_e , the number of aliquots, over dispersion values are shown in Figure 4 and summarized in Table 3.

Effects of signal composition on D_e

The post-IR OSL signals are shown in Fig.5. We observed that the luminescence efficiency varied between aliquots; and the aliquots showing high luminescence efficiency showed a contribution from other components than the fast component. The corresponding growth curves were fitted using

than the fast OSL component. Fitting results on 23 single aliquots of sample MOR3 revealed that only 4 aliquots comprised the dominant fast OSL component.

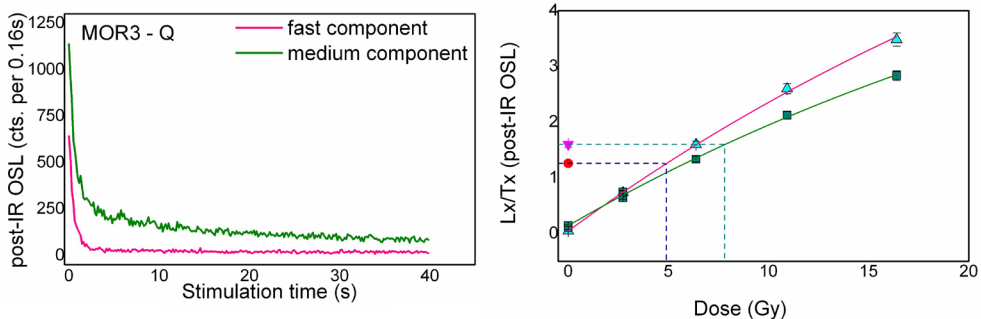


Figure 5. post-IR OSL signal, fast component (red) and medium component (green)

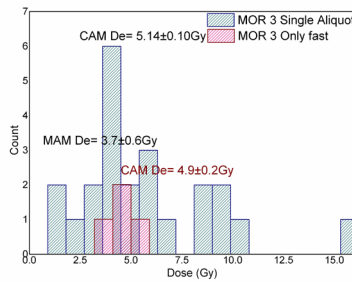


Figure 6. Dose distributions for quartz sample MOR3: all D_e estimates are shown blue and D_e derived only from fast components is shown red

Figure 6 shows dose distributions as histograms for all dose estimates (blue) and for D_e derived from fast component comprising 4.9 ± 0.2 Gy.

DISCUSSION AND CONCLUSION

For the site MOR-3 single grain analysis failed due to dim signals, it was not possible to carry out reliable single grain measurements for the young sample under study. The small-aliquots comprise of 100 grains from which up to 3-4 grains might contribute to the dose estimate. Furthermore, the small-aliquots showed an infrared signal relating either to the presence of feldspar (REF) or to the medium OSL component. TL peak around 200°C which is indicative for feldspar was apparent for grains showing a dominant medium

component.

D_e distributions of post-IRSL OSL measurements on quartz were highly over-dispersed: the CAM D_e is 5.14 ± 0.10 Gy with OD of 47.5%. To improve the accuracy of the D_e estimation, the acceptance criteria based on the precision on D_e were applied and the most precise 11 aliquots yield the CAM D_e of 4.21 ± 0.22 Gy and OD of 13.3%. Because of this apparent discrepancy further statistical analysis were made.

Table 3. Summary of dose, dose rate and age results for samples. The selected D_e and ages are indicated bold

MOR-3	$\sigma D_e < 30\%$	$\sigma D_e < 20\%$	$\sigma D_e < 10\%$	De from fast OSL
N aliquots	23	20	11	4
CAM D_e , Gy	5.14 ± 0.1	4.37 ± 0.3	4.21 ± 0.22	4.9 ± 0.2
OD, %	47.5	40.2	17.7	10.3
MAM D_e , Gy	3.7 ± 0.6	-	-	-
Dr, Gy/ka	3.99 ± 0.17			
MAM age, (years)	930 ± 80 (1090 AD)	-	-	-
CAM age, (years)	1290 ± 70 (725 \pm 70 AD)	1100 ± 100 (920 \pm 100 AD)	1055 ± 80 (960 \pm 80 AD)	1230 ± 80 (785 \pm 80 AD)

Statistical models are powerful at revealing the incomplete bleaching and post-depositional mixing or disturbance [11] which might result in distinct dose populations. Post-depositional disturbance may be discounted if sedimentary structures or layering are preserved. But such features are not always evident, especially at archaeological sites because of anthropogenic activities [19]. Assuming an incomplete bleaching at the deposition and applying the minimum dose model, we obtained the MAM dose of 3.7 ± 0.6 Gy.

In contrast, signal composition of the post-IR OSL through fitting revealed that the initial signal was dominated by fast or medium components. Signals dominated by the medium component yield higher luminescence efficiency and give higher dose estimates than the fast components. Based on the accepted $n=4$ aliquots showing the fast component dominated signal, we obtain D_e of 4.9 ± 0.2 Gy.

This apparent discrepancy between the D_e obtained from the fast component and D_e obtained from the most precise dose estimates means that the most precise estimates were derived from the aliquots showing other components than the fast OSL, which are much brighter and consequently have error on the D_e estimate $<10\%$. The dose D_e obtained from the fast OSL is consistent with CAM D_e

derived with precision on $D_e < 30\%$.

Summary of the luminescence results are shown in Table 3.

We conclude that

1. Small-aliquots as proxy single-grain measurements gave an opportunity to compare the doses evaluated using two different approaches, namely the statistical modeling and signal composition analysis.

2. The signal composition analysis is reliable due to the well-known signal parameters of blue stimulated fast and medium components. It revealed that the brighter grains with different luminescence characteristics may yield higher doses which were erroneously accepted due to high precision by using the statistical modeling. Further analysis of single grains and analysis of fast and medium components is needed to verify the findings and to improve the accuracy of dose estimation.

3. The walled enclosure MOR 3 was constructed not as expected during the 906-1125 AD based on the archaeological evidence, but during 785 ± 80 AD. In addition, the possibility of rebuilding, reusing or collapse of the ramparts during the 1090 ± 80 AD cannot be ruled out due to the MAM age of 930 ± 80 years.

Acknowledgements

The luminescence measurements were conducted at luminescence laboratory Köln. Tengis's work was financed by the research grant from the Mongolian Science and

Technology Foundation. Research stay of Saran Solongo was financed by DAAD. The anonymous reviewer is thanked for providing constructive comments.

REFERENCES

1. Adamiec, G., A. Bluszcz, R. Bailey, and M. Garcia-Talavera, Finding model parameters: Genetic algorithms and the numerical modelling of quartz luminescence. *Radiation Measurements*, 2006. **41**(7–8): p. 897-902.
2. Aitken, M.J., *An introduction to optical dating. The dating of Quaternary sediments by the Use of Photon-Stimulated Luminescence 1998: Oxford, New York, Tokyo: Oxford University Press.*
3. Bailey, R.M., B.W. Smith, and E.J. Rhodes, Partial bleaching and the decay form characteristics of quartz OSL. *Radiation Measurements*, 1997. **27**(2): p. 123-136.
4. Bailey, R.M., E.G. Yukihara, and S.W.S. McKeever, Separation of quartz optically stimulated luminescence components using green (525 nm) stimulation. *Radiation Measurements*, 2011. **46**(8): p. 643-648.
5. Banerjee, D., A.S. Murray, L. Bøtter-Jensen, and A. Lang, Equivalent dose estimation using a single aliquot of polymineral fine grains. *Radiation Measurements*, 2001. **33**(1): p. 73-94.
6. Bemann, J., B. Ahrens, C. Grütznier, R. Klinger, N. Klitzsch, F. Lehmann, S. Linzen, L. Munkhbayar, G. Nomguunsuren, M. Oczipka, H. Piezonka, B. Schütt, and S. Saran, Geoaerchaeology in the steppe: first results of the multidisciplinary Mongolian-German survey project in the Orkhon valley, central Mongolia. *Studia Archaeologica Instituti Archaeologici Academiae Scientiarum Mongolicae*, XXX, Fasciulus, 2011.
7. Bøtter-Jensen, L., S. Solongo, A.S. Murray, D. Banerjee, and H. Jungner, Using the OSL single-aliquot regenerative-dose protocol with quartz extracted from building materials in retrospective dosimetry. *Radiation Measurements*, 2000. **32**(5–6): p. 841-845.
8. Duller, G.A.T., Improving the accuracy and precision of equivalent doses determined using the optically stimulated luminescence signal from single grains of quartz. *Radiation Measurements*, 2012. **47**(9): p. 770-777.
9. Fattahi, M., M. Heidary, and M. Ghasemi, Employing Minimum age model (MAM) and Finite mixture modeling (FMM) for OSL age determination of two important samples from Ira Trench of North Tehran Fault, in *Geochronometria*. 2016. p. 38.
10. Galbraith, R.F. and R.G. Roberts, Statistical aspects of equivalent dose and error calculation and display in OSL dating: An overview and some recommendations. *Quaternary Geochronology*, 2012. **11**: p. 1-27.
11. Galbraith, R.F., R.G. Roberts, G.M. Laslett, H. Yoshida, and J.M. Olley, Optical Dating of Single and multiple grains of quartz from jinnium rock shelter, northern Australia: part I, Experimental Design and statistical models. *Archaeometry*, 1999. **41**(2): p. 339-364.
12. Guerin, G., N. Mercier, and G. Adamiec, Dose-rate conversion factors: update. 2011, *Ancient TL*. p. 5-8.
13. Jacobs, Z., G.A.T. Duller, and A.G. Wintle, Interpretation of single grain distributions and calculation of. *Radiation Measurements*, 2006. **41**(3): p. 264-277.
14. Nathan, R.P., P.J. Thomas, M. Jain, A.S. Murray, and E.J. Rhodes, Environmental dose rate heterogeneity of beta radiation and its implications for luminescence dating: Monte Carlo modelling and experimental validation. *Radiation Measurements*, 2003. **37**(4): p. 305-313.
15. Olley, J., G. Caitcheon, and A. Murray, The distribution of apparent dose as determined by Optically Stimulated Luminescence in small aliquots of fluvial quartz: Implications for dating young sediments. *Quaternary Science Reviews*, 1998. **17**(11): p. 1033-1040.
16. Prescott, J.R. and J.T. Hutton, Cosmic ray contributions to dose rates for luminescence and ESR dating: Large depths and long-term time variations. *Radiation Measurements*, 1994. **23**(2–3): p. 497-500.



17. Preusser, F., M.L. Chithambo, T. Götze, M. Martini, K. Ramseyer, E.J. Sendezera, G.J. Susino, and A.G. Wintle, *Quartz as a natural luminescence dosimeter. Earth-Science Reviews*, 2009. **97**(1–4): p. 184-214.
18. Roberts, R.G., *Luminescence dating in archaeology: from origins to optical. Radiation Measurements*, 1997. **27**(5): p. 819-892.
19. Roberts, R.G., Z. Jacobs, B. Li, N.R. Jankowski, A.C. Cunningham, and A.B. Rosenfeld, *Optical dating in archaeology: thirty years in retrospect and grand challenges for the future. Journal of Archaeological Science*, 2015. **56**: p. 41-60.
20. Saran, S., S. Tengis, and B. Tsogtbaatar, *WHAT THE BRICKS TELL US FROM A TEMPLE AT BURKHAN KHALDUN MOUNTAINS: CHRONOLOGICAL INSIGHTS FROM pIRIR LUMINESCENCE. Proceedings of the Mongolian Academy of Sciences*, 2016. **4**: p. 4-12.
21. Saran, S., G.A. Wagner, and T. Galbaatar, *The chronology of brick manufacturing at the Kharakhorum, Mongolia. Preprints of the Institute of Physics and Technology, MAS*, 2006. **33**: p. 60-64.
22. Solongo, S., D. Richter, B. Tuguldur, and J.J. Hublin, *OSL and TL characteristics of fine grain quartz from Mongolian prehistoric pottery used for dating. Geochronometria*, 2014. **41**(1): p. 15-23.
23. Solongo, S., S. Tengis, N. Erdene-Ochir, and J.-J. Hublin, *Testing the pIRIR on pottery and SG-OSL on clay sediment from the known age Xiongnu "Royal" tomb at Noin Ula, Mongolia. Archaeological and Anthropological Sciences*, 2017.
24. Solongo, S., G.A. Wagner, and T. Galbaatar, *The estimation of using the fast and medium components in fired quartz from archaeological site Karakorum, Mongolia. Radiation Measurements*, 2006. **41**(7–8): p. 1001-1008.
25. Wintle, A.G. and A.S. Murray, *A review of quartz optically stimulated luminescence characteristics and their relevance in single-aliquot regeneration dating protocols. Radiation Measurements*, 2006. **41**(4): p. 369-391.